Original Article

Resveratrol Nanoparticle Pretreatment Improved the Oral Bioavailability of Bromocriptine: Involvement of Liver and Intestinal CYP3A Enzyme Inhibition

Prasad Neerati, Suresh Palle[1]

Departments of Pharmacology and [1]Toxicology DMPK and Clinical Pharmacology Division, University College of Pharmaceutical Sciences, Kakatiya University, Warangal, Telangana, India

Abstract

Background: Resveratrol (RSV) is a polyphenol belonging to phytoalexin family and has been reported to show inhibitory effects on CYP3A4 enzymes. However, there has been no report about the pharmacokinetic interaction of bromocriptine (BRO) with RSV and RSV nanoparticles (NRSV) in rats. Hence, the present study was undertaken in an attempt to enhance the oral bioavailability of BRO when BRO was pretreated with RSV and NRSV. **Materials and Methods:** Antisolvent precipitation method is used to prepare NRSV under temperature control. The following methods were used in this study, i.e., *in vitro* assessment of CYP3A activity in liver and intestinal microsomes and *in vitro* noneverted sac method. To confirm the *in vitro* findings, an *in vivo* pharmacokinetic study was also performed. **Results:** The results indicate that RSV significantly ($P < 0.05$) inhibited the CYP3A activity in intestinal and liver microsomes. In noneverted sac study, the intestinal transport and P_{app} of BRO were more significant ($P < 0.05$) in NRSV as compared to RSV group. Further, *in vivo* study revealed that the increased levels of C_{max} and AUC were comparatively higher in NRSV-pretreated group than RSV group. In addition, pretreatment with RSV and NRSV significantly ($P < 0.05$) decreased the mean appararant clearance (CL/F) of BRO. **Conclusion:** NRSV pretreatment significantly increased the intestinal absorption and bioavailability of BRO probably by the inhibition of CYP3A-mediated metabolism in rats. However, further studies are needed to confirm these interactions in humans.

Keywords: Bromocriptine, CYP3A, high-performance liquid chromatography, oral bioavailability, resveratrol nanoparticles

Introduction

Resveratrol (RSV) is a polyphenol belonging to the phytoalexin family, abundantly present in fruits, vegetables, grapes, peanuts, and blueberries.[1] RSV possesses diverse biochemical and physiological properties including antioxidative stress,[2] anti-inflammation, and anti-carcinogenic activities[3] as well as neuroprotective effects.[4] Previous *in vitro* and *in vivo* studies demonstrated that RSV is an inhibitor of cytochrome P450 (CYP) 3A4,[5,6] and it inactivates the enzyme in the presence of nicotinamide adenine dinucleotide phosphate (NADPH).[7,8] In addition, RSV and its metabolite RSV-3-sulfate have been reported as inhibitors of CYP3A.[9]

From the literature, it is evident that RSV is practically water insoluble and has low bioavailability.[10] Hence, clinical application of this drug greatly restricted. In this regard, to circumvent the problems of poor bioavailability and poor pharmacokinetics associated with RSV, several strategies such as nanoparticles, liposomes, and nanoemulsions have been developed by performing extensive studies.[11] According to the Noyes and Whitney equation, particle size reduction effectively increases the surface area of poorly water-soluble compounds and therefore enhances the solubility and dissolution rate.[12] Nanoparticle technology is an excellent drug delivery system developed to enhance the saturation solubility and bioavailability of many therapeutic drugs, especially highly hydrophobic agents like RSV.

Access this article online

Quick Response Code:

Website: www.jnsbm.org

DOI: 10.4103/jnsbm.JNSBM_126_19

Address for correspondence: Dr. Prasad Neerati, Department of Pharmacology, DMPK and Clinical Pharmacology Division, University College of Pharmaceutical Sciences, Kakatiya University, Warangal, Telangana, India.
E-mail: prasadneerati@gmail.com

How to cite this article: Neerati P, Palle S. Resveratrol nanoparticle pretreatment improved the oral bioavailability of bromocriptine: Involvement of liver and intestinal CYP3A enzyme inhibition. J Nat Sc Biol Med 2019;10:209-16.

The CYP3A4 is one of the most important subfamily of CYP isoforms found in critical tissues such as the liver and intestine.[13,14] CYP3A4 enzymes are responsible for first-pass metabolism and changes in absorption, distribution, and metabolism of orally administered many drugs.[15,16] Therefore, inhibition of CYP3A4 activity greatly impacts the bioavailability of orally administered drugs which are substrates for this enzyme.

Bromocriptine (BRO) a semisynthetic derivative of ergot alkaloid, is an agonist of dopamine receptor, and directly and indirectly protects dopaminergic cells. BRO is widely used in the treatment of pituitary tumors, breast tumors, hyperprolactinemia, infertility, menstrual disorders, type 2 diabetes, and especially in Parkinson's disease.[17-19] BRO is available in tablet and capsule dosage form; it is easily absorbed through the gastrointestinal tract, but due to extensive first-pass metabolism, only 3%–5% of the ingested dose reaches the systemic circulation.[20,21] BRO is a substrate of CYP3A4, extensively metabolized in the gastrointestinal tract and liver by the CYP3A4 cytochrome system.[22] Potent inhibitors or inducers of CYP3A4 may increase or reduce the circulating levels of BRO.[23] Therefore, oral administration of BRO with coadministered substances such as RSV and RSV nanoparticles (NRSV) could improve the efficacy and allow the optimal therapeutic dosing.

However, there has been no report about the pharmacokinetic interaction of BRO with RSV and NRSV in rats. Hence, the present study was undertaken in an attempt to enhance the oral bioavailability of BRO when BRO was pretreated with RSV and NRSV.

Rats were chosen as an animal model to investigate the pharmacokinetic interaction of BRO with RSV and NRSV although there should be some extent of difference in CYP enzyme activity between rat and human.[24] The influence of RSV and NRSV on the pharmacokinetics of BRO was evaluated *in vivo* by assessment of CYP3A activity in liver and intestinal microsomes. The intestinal permeability characteristics of BRO were mechanistically investigated using the *in vivo* noneverted sac method. To confirm these findings, an *in vivo* pharmacokinetic study of orally administered BRO in rats with RSV and NRSV pretreatments was performed.

Materials and Methods

Materials

BRO was kindly donated by Inga laboratories Pvt. Ltd., Maharashtra, India. RSV, purchased from Sigma–Aldrich (USA), the absolute ethanol (99.5%–99.8%), and acetonitrile (high-performance liquid chromatography [HPLC] grade) were obtained from Merck, Mumbai, India. Water for analytical purpose is double-distilled, filtered using direct-Quv millipore, and sonicated for removing air bubbles. All other reagents used were also of analytical grade.

Preparation of resveratrol nanoparticles

The NRSV were prepared by temperature-controlled antisolvent precipitation method using syringe pump.[25] RSV was dissolved in the solvent ethanol and prepared a solution at a predetermined concentration of 60 mg/mL. The obtained organic solution was added to precooled (5°C) antisolvent (deionized water) in a drop-wise manner under rapid magnetic stirring at 1000 rpm. The formed NRSV was filtered and vacuum-dried.

Particle morphology

The particle size and morphology of samples were observed using a scanning electron microscope (SEM) Zeiss EVO 18-EDX special edition machine compatible with energy dispersive X-ray (EDX) machine. The powder samples were spread on a SEM stub and sputtered with gold before the SEM observations. The particle size and texture of nanoparticles can be analyzed using image magnification software compatible with SEM and helps in determining the presence and formation of NRSV. Five SEM pictures were used to find the average range of particle diameter.

In vitro dissolution testing

The *in vitro* dissolution of the prepared NRSV samples, as well as the original RSV, was determined using the paddle method (USP 29 type II) (Electro Lab, TDT 06P) in 100 mL of simulated intestinal fluid (SIF, pH 6.8). The rotation speed of paddle was set at 100 rpm, and the bath temperature was kept at 37°C ± 0.5°C. The original RSV and NRSV containing 5 mg of sample were tested for their dissolution in simulated intestinal fluid.[26] Samples of 1 mL volume were collected at 15, 30, 45, 60, 90, 120, and 180 min of dissolution time. The dissolution test for each sample was performed in triplicate, and the dissolution data were averaged. The absorbance was measured at 308 nm using ultraviolet (UV) spectrometer.

Animals

Male albino Wistar rats (180–250 g) were used for the study. The rats were kept in polyacrylic cages and maintained under standard laboratory conditions (room temperature24°C–27°C and humidity 60%–65%). Each experimental group consisted of six animals that were chosen randomly from different cages. Handling and experimentation were conducted in accordance with the approved guidelines of the Committee for the Purpose of Control and Supervision of Experiments on Animals, New Delhi, and the experimental protocol was approved by Institutional Animal Ethical Committee (IAEC) Kakatiya University. Approval no: IAEC/06/UCPSC/KU/16.

In vitro assessment of CYP3A activity

An *in vitro* CYP3A activity was performed according to the previously described method.[27] This method is based on the principle of CYP3A converts erythromycin to *N*-demethyl erythromycin and formaldehyde, which produced yellow color with Nash reagent.[28]

Preparation of intestinal microsomes

The intestinal microsomes were prepared by slight modification of previously reported methods.[29,30] The isolated intestine was

cut into pieces, washed with ice-cold phosphate-buffered saline and then cut longitudinally to expose mucosa. The mucosal layer was scraped lightly from all pieces of intestine with the help of a cover slip. All scrapings were mixed together and centrifuged at 25 × g for 5 min. The pellet was suspended in 5.0 mL of ice-cold histidine–sucrose buffer (HSB) (histidine 5 mM, pH 7.0; sucrose 0.25 M; NaEDTA 0.5 mM; pH 7.4); homogenized and centrifuged at 15,000 × g for 10 min. The supernatant was carefully transferred to a clean tube. The pellet was resuspended in 5.0 mL of HSB and again centrifuged at 15,000 × g for 10 min. The supernatant after each centrifugation was taken together and mixed with 52 mM CaCl2 (0.2 mL per mL of the supernatant) to precipitate microsomes. After 15 min of standing, it was centrifuged at 20,000 × g for 15 min, the microsomal pellet was suspended in 0.5 mL of 0.1 M potassium phosphate buffer containing 20% glycerol, and stored at − 20°C until needed. The protein concentration of the microsomal fraction was determined by Biuret method using bovine serum albumin as the standard.

Preparation of liver microsomes

The liver microsomes were prepared by slight modification of previously reported method.[31] The liver isolated from rats was minced and homogenized in 5 mL of 0.25 M sucrose containing 10 mM Tris-HCl (pH 7.4) and then centrifuged at 600 × g for 5 min followed by 12,000 × g for 10 min. The postmitochondrial supernatant was separated, mixed with 52 mM $CaCl_2$ (0.2 mL per mL of the supernatant) to precipitate microsomes. After 15 min of standing, it was centrifuged at 20,000 × g for 15 min; the microsomal pellet was suspended in mixture of 150 mM KCl-10 mM Tris-HCl, and centrifuged at 20,000 × g for 20 min to obtain pinkish microsomal pellet, which was suspended in 0.5 mL of 0.1 M potassium phosphate buffer containing 20% glycerol, and stored at −20°C until needed.

Erythromycin-N-demethylation assay

The mixture of microsomal suspension (0.1 mL, 25%), erythromycin (0.1 mL, 10 mM), and potassium phosphate (0.6 mL, 100 mM, pH 7.4) was incubated at 37 ˚C along with RSV at a concentration of 0.1, 1, and 10 µM. The reaction between these agents was initiated by adding NADPH (0.1 mL, 10 mM), and terminated after 10 min, by adding ice-cold trichloroacetic acid (0.5 mL, 12.5% w/v) solution. It was centrifuged (2000 × g; 10 min) to remove proteins. To 1 mL of this supernatant, 1 mL of Nash Reagent (2 M ammonium acetate, 0.05 M glacial acetic acid, and 0.02 M acetyl acetone) was added and heated in a water bath at 50°C for 30 min. After cooling, the absorbance was read at 412 nm. The activity was calculated from standards (1–100 µM formaldehyde) prepared by substituting sample with the standard solution which was run in parallel. The CYP3A activity was expressed as µM of formaldehyde obtained per milligram of protein per hour.

In vitro noneverted intestinal sac study

An *in vitro* noneverted intestinal sac study was performed according to the previously described methods.[32,33] The rats were divided into three groups control, RSV and NRSV each consisting of six animals. RSV and NRSV were administered orally at a dose of 40 mg/kg for 10 days, and other group was kept as control without any drug treatment. All the animals were sacrificed on 11th day, and the intestine was surgically removed and flushed with 50 mL of ice-cold saline. The small intestine was cut into 3 segments, duodenum, jejunum, and ileum of equal length (5 cm). The probe drug (BRO 500 µg/mL) was dissolved in pH 7.4 isotonic Dulbecco's PBS (D-PBS) containing 25 mM glucose. The probe drug solution (1 mL) was filled in the normal sac (mucosal side), and both ends of the sac were ligated tightly. The sac containing probe drug solution was placed in a beaker containing 40 mL of D-PBS, containing 25 mM glucose. The medium was prewarmed at 37°C and preoxygenated with 5% CO_2/95% O_2 for 15 min, under bubbling with a CO_2/O_2 mixture gas; the transport of the BRO from mucosal to serosal direction across the intestinal sacs was measured by sampling the serosal medium periodically for 120 min. The samples of 1 mL were collected from intestinal sacs of control, RSV, and NRSV rats at predetermined time points and stored at −80°C until analysis. The drug transported from mucosal to serosal direction was measured by HPLC.

Calculation of apparent permeability coefficient

The apparent permeability coefficient (P_{app}) of BRO was calculated from the following equation:[34]

$$Papp = \frac{dQ}{dt} \cdot \frac{1}{AC0}$$

Where dQ/dt is the transport rate of drug in the serosal medium, A is the surface area of the intestinal sacs, and C_0 is the initial concentration inside the sacs.

In vivo pharmacokinetic study

Rats were fasted for at least 24 h before experiments and approximately 3-h postdose. The rats were divided into 3 groups consisting of six animals each. Group I was administered with BRO (10 mg/kg; p.o.) on the 11th day. Group II was pretreated with RSV (40 mg/kg; p.o.) for 10 days and on the 11th day with BRO (10 mg/kg) followed by RSV, and Group III was pretreated with NRSV (40 mg/kg; p.o.) for 10 days and on the 11th day with BRO (10 mg/kg) followed by NRSV. Blood samples (approximately 0.25 mL) were collected from subclavian vein at specified time intervals, then placed into heparinized tubes and separated immediately by centrifugation (15000 rpm for 15 min). The plasma samples obtained were stored at −80°C until the HPLC analysis.

High-performance liquid chromatography analysis of bromocriptine

The drug analysis of samples was carried out using Shimadzu HPLC system equipped with a LC-20AD pump, SPD 20A UV visible detector, Rheodyne injector port (20 µL loop) and RP C18 column (Phenomenex Luna, 250 mm × 4.6 mm ID, particle size 5 mm). The mobile phase comprised of acetonitrile water (0.2% triethylamine) (70:30 v/v), adjusted to pH 3 with HCL. Analyses were run at a flow rate of 1 mL/min, and the elution was monitored at 280 nm.[35]

In vitro and plasma samples were extracted using a simple protein precipitation method by adding acetonitrile (200 µL) to samples (100 µL). Samples vortexed for 2 min and centrifuged at 15,000 rpm for 15 min. The resultant clean supernatant (20 µL) was injected and analyzed using HPLC method. The limit of detection was 0.01 µg/mL, and the assay range used was 0.01–10 µg/mL. The average recovery of the drug was 91.7%. The intra- and inter-day coefficients of variation for the low and high quality control samples were <10%.

Pharmacokinetic analysis

Pharmacokinetic parameters were computed by the noncompartmental model using Phoenix WinNonlin version 6.2 software (Certara, Pharsight Corporation, USA). The maximum plasma concentration (C_{max}) and the time to reach the maximum plasma concentration (t_{max}) were determined by a visual inspection of the experimental data. The plasma BRO concentration versus time plots were used to estimate the area under the concentration–time curve to the last sampling point (AUC_{0-t}), area under the concentration–time curve to the infinity ($AUC_{0-\infty}$), half-life ($t_{1/2}$), elimination rate constant (k_{el}), and clearance (CL/F).

Statistical analysis

All mean values are presented as with their standard deviation (SD) (mean ± SD). Significant difference between means was evaluated by one-way analysis of variance followed by Bonferroni multiple comparison tests, $P < 0.05$ was considered as statistically significant.

Results

Resveratrol nanoparticles characterization by scanning electron microscope

SEM micrographs of the RSV and NRSV are shown in Figure 1a and b. It is observed that the RSV powder Figure 1a exhibited particles lacking uniformity in size and was much larger than the NRSV Figure 1b. On the other hand, NRSV prepared by syringe pump exhibited particles uniformity in size, less crystallinity, and absence of larger particles Figure 1b. As depicted in the image, the particles possessed uniform shape. The size of all particles was found to be within the range of 100–250 nm.

In vitro dissolution

The dissolution profiles of the commercial RSV and the formulated NRSV in simulated intestinal fluid SIF at pH 6.8 shown in Figure 1c. NRSV were dissolved 90% at 180 min. On the other hand, 58% of the commercial RSV was dissolved in the same period. It was observed that NRSV reached 50% dissolution in 45 min whereas the commercial RSV reached 50% dissolution at 120 min.

Assessment of *in vitro* CYP3A activity in intestinal microsomes

The extent of erythromycin-N-demethylation (EMD) due to CYP3A activity in intestinal microsomes is shown in Figure 1d. The EMD levels in RSV-treated group at all concentrations 0.1, 1, and 10 µM were significantly reduced ($P < 0.05$) when compared with vehicle.

Assessment of *in vitro* CYP3A activity in liver microsomes

The extent of EMD due to CYP3A activity in liver microsomes is shown in Figure 1e. RSV treatment significantly decreased $P < 0.05$ EMD levels at 1 µM and 10 µM while it has no significant effect at 0.1 µM.

Effect of resveratrol and resveratrol nanoparticles on intestinal transport and apparent permeability of bromocriptine

The present investigation involves the determination of BRO intestinal transport and P_{app} in control, RSV, and RSVN treatment groups. Pretreatment with RSV (40 mg/kg) for 10 days resulted in a significant ($P < 0.05$) increase in mean cumulative concentrations from mucosal to serosal direction of BRO from 9.45 ± 0.87 to14.27 ± 0.74 µg/mL in duodenum; 7.29 ± 0.62–12.78 ± 0.86 µg/mL in jejunum; and 5.25 ± 0.36–11.72 ± 0.75 µg/mL in ileum Figure 1f. In addition, pretreatment with NRSV (40 mg/kg) for 10 days resulted in a significant ($P < 0.05$) increase in mean cumulative concentrations from mucosal to serosal direction of BRO from 9.45 ± 0.87–18.65 ± 0.54 µg/mL in duodenum; 7.29 ± 0.62–16.53 ± 0.69 µg/mL in jejunum; and 5.25 ± 0.36–14.81 ± 0.62 µg/mL in ileum.

The transport of BRO was found to be increased by 1.5-, 1.7- and 2.2-fold in duodenum, jejunum and ileum, respectively, in RSV-pretreated group when compared with the BRO alone group. Further, the transport of BRO was found to be increased by 1.9-, 2.2- and 2.8-fold in duodenum, jejunum, and ileum, respectively, in RSVN-pretreated group when compared with the BRO alone group. Pretreatment with RSV resulted in a significant $P < 0.05$) increase in P_{app} of BRO from $0.313 \pm 0.063 \times 10^{-4}$ to $0.683 \pm 0.056 \times 10^{-4}$ cm/s in duodenum; $0.269 \pm 0.042 \times 10^{-4}$–$0.594 \pm 0.043 \times 10^{-4}$ cm/s in jejunum; and $0.203 \pm 0.026 \times 10^{-4}$–$0.539 \pm 0.034 \times 10^{-4}$ cm/s in ileum Figure 1g. In addition, pretreatment with NRSV resulted in a significant ($P < 0.05$) increase in P_{app} of BRO from $0.203 \pm 0.026 \times 10^{-4}$ to $0.649 \pm 0.032 \times 10^{-4}$ cm/s in duodenum; $0.269 \pm 0.042 \times 10^{-4}$–$0.693 \pm 0.042 \times 10^{-4}$ cm/s in jejunum; and $0.313 \pm 0.063 \times 10^{-4}$–$0.783 \pm 0.053 \times 10^{-4}$ ileum Figure 1g. The P_{app} of BRO in duodenum, jejunum, and ileum was found to be increased by 2.1-, 2.2-, and-2.6-fold, respectively, in RSV-pretreated group when compared with BRO alone group. Whereas in case of RSVN-pretreated group, the P_{app} of BRO in duodenum, jejunum, and ileum was found to be increased by 2.5, 2.5, and 3.2 fold, respectively, when compared with BRO alone group. The increased intestinal transport and P_{app} of BRO were more prominent in RSVN-pretreated group than the RSV-pretreated group.

Effect of resveratrol and RSVN on pharmacokinetics of bromocriptine

The effects of RSV and NRSV (40 mg/kg, p.o.) on the plasma concentration–time plots of orally administered

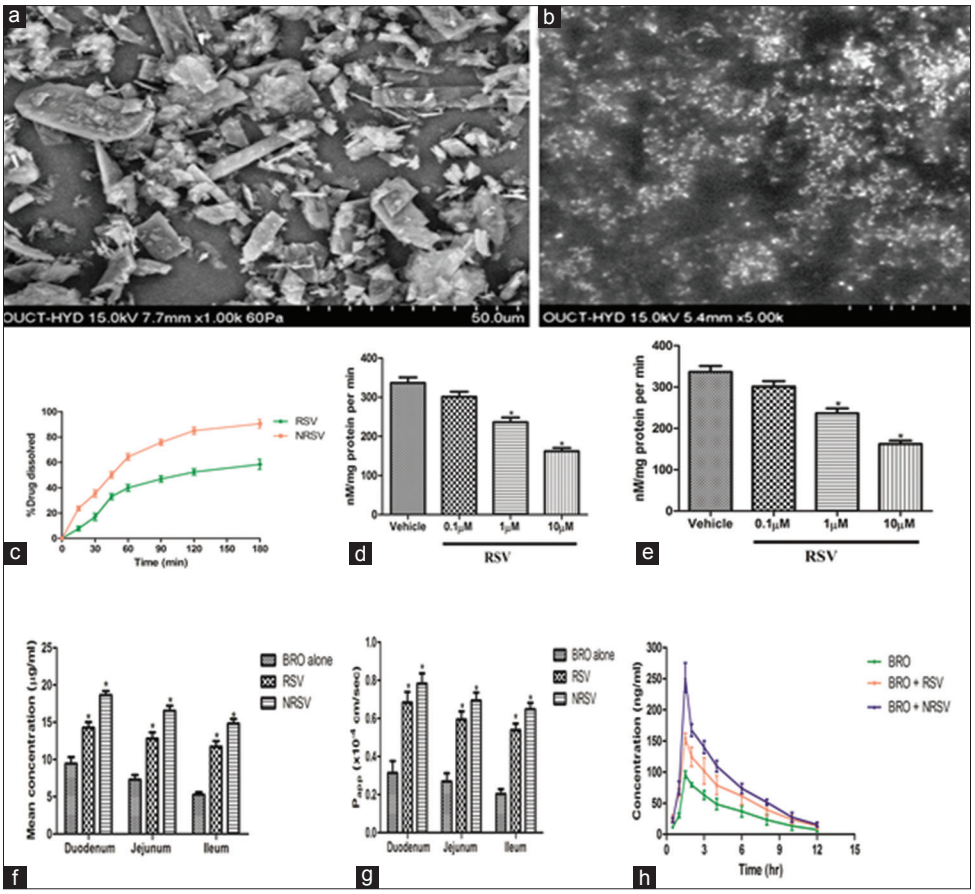

Figure 1: Scanning electron microscope photographs of (a) resveratrol and (b) resveratrol nanoparticles. (c) Dissolution profile of commercial resveratrol and resveratrol nanoparticles. (d) Effect of resveratrol on *in vitro* CYP3A activity in intestinal microsomes. Data are represented as mean ± standard deviation ($n = 6$). *Significant difference ($P < 0.05$) in comparison with the vehicle. Statistical analysis was carried out using one-way analysis of variance followed by Bonferroni multiple comparisons test. (e) Effect of resveratrol on *in vitro* CYP3A4 activity in liver microsomes. Data are represented as mean ± standard deviation $n = 6$). *Significant difference ($P < 0.05$) in comparison with the vehicle. Statistical analysis was carried out using one-way analysis of variance followed by Bonferroni multiple comparisons test. (f). Intestinal transport of bromocriptine in duodenum, jejunum, and ileum of Wistar rats. Data are represented as mean ± standard deviation ($n = 6$). *Significant difference ($P < 0.05$) in comparison with the bromocriptine alone. Statistical analysis was carried out using two-way analysis of variance followed by Bonferroni multiple comparisons test. (g) Apparent permeability coefficient (P_{app}) of bromocriptine in duodenum, jejunum, and ileum of Wistar rats. Data are represented as mean ± standard deviation ($n = 6$). *Significant difference ($P < 0.05$) in comparison with the bromocriptine alone. Statistical analysis was carried out using two-way analysis of variance followed by Bonferroni multiple comparisons test. (h) Plasma drug concentration–time plots of bromocriptine (10 mg/kg) in Wistar rats. Control group administered with bromocriptine alone on 11th day and pretreatment groups administered with resveratrol and NRSV for 10 days and on the 11th day with bromocriptine followed by resveratrol and resveratrol nanoparticles. Data are represented as mean ± standard deviation ($n = 6$)

BRO (10 mg/kg, p.o.) were characterized and depicted in Figure 1h, and the pharmacokinetic parameters were summarized in Table 1. RSV and RSVN pretreatment for 10 days significantly ($P < 0.05$) altered the pharmacokinetics of oral BRO when compared with the control group BRO alone. The C_{max}, AUC_{0-t}, and $AUC_{0-\infty}$ of BRO were found to be increased by 1.6, 1.66, and 1.69 fold, respectively, in RSV-pretreated group when compared with the control group. The C_{max}, AUC_{0-t} and $AUC_{0-\infty}$ of BRO were found to be increased by 2.62, 2.18, and 2.21 fold, respectively, in NRSV-pretreated group when compared with the control group. Further, the CL/F of BRO was significantly decreased while there was no significant change observed in t_{max} of BRO in RSV and RSVN-pretreated groups when compared with control group. The changes in pharmacokinetic parameters of BRO were more prominent in RSVN-pretreated group than the RSV-pretreated group.

Effect of resveratrol and resveratrol nanoparticles on pharmacokinetics of bromocriptine

The effects of RSV and NRSV (40 mg/kg, p. o.) on the plasma concentration–time plots of orally administered BRO (10 mg/kg, p. o.) were characterized and depicted in Figure 1, and the pharmacokinetic parameters were summarized in Table 1. RSV and NRSV pretreatment for 10 days significantly ($P < 0.05$) altered the pharmacokinetics of oral BRO when compared with the control group (BRO alone). The C_{max}, AUC_{0-t}, and $AUC_{0-\infty}$ of BRO were found to be increased by 1.6, 1.66, and 1.69 fold, respectively, in RSV-pretreated group when compared with the control

Table 1: Pharmacokinetic parameters of bromocriptine in control, resveratrol, and pretreated group rats after oral administration of 10 mg/kg postoperative bromocriptine

Pharmacokinetic parameters	BRO	BRO + RSV	BRO +
C_{max} (ng/mL)	96.02±5.65	153.74±8.51*	251.71±23.55*
t_{max} (h)	1.5±0	1.5±0	1.5±0
AUC_{0-t} (h ng/mL)	417.55±78.05	693.75±109.25*	913.27±67.85*
$AUC_{0-\infty}$ (h ng/mL)	442.63±86.20	748.56±121.33*	978.98±91.44*
k_{el} (h^{-1})	0.29±0.03	0.27±0.05	0.26±0.03
$t_{1/2}$ (h)	2.39±0.19	2.65±0.51	2.72.0±0.35
CL/F (L/h)	23.25±4.07	13.73±2.74*	10.29±0.95*

Data values are presented as mean±SD (n=6). *Significant difference (P<0.05) in comparison with the control. BRO: Bromocriptine, RSV: Resveratrol, SD: Standard deviation, C_{max}: Maximum plasma concentration, t_{max}: Time to reach the maximum plasma concentration, AUC_{0-t}: Area under the concentration–time curve to the last sampling point, $AUC_{0-\infty}$: Area under the concentration–time curve to the infinity, k_{el}: Elimination rate constant, $t_{1/2}$: Half- life, CL/F: Clearance

group. The C_{max}, AUC_{0-t}, and $AUC_{0-\infty}$ of BRO were found to be increased by 2.62, 2.18, and 2.21 fold, respectively, in NRSV-pretreated group when compared with the control group. Further, the CL/F of BRO was significantly decreased while there was no significant change observed in t_{max} of BRO in RSV and NRSV-pretreated groups when compared with control group. The changes in pharmacokinetic parameters of BRO were more prominent in NRSV-pretreated group than the RSV-pretreated group.

Discussion

Herbal constituents have the greatest potential to modulate the expression and activity of drug-metabolizing enzymes, such as cytochromes P450, leading to clinically significant herb–drug interactions as they can affect the absorption and disposition of concomitantly administered drugs.[36,37] Hence, it is best known that pharmacokinetic herb–drug interactions have attracted attention by the patients and healthcare professionals due to their improved therapeutic benefits.[38]

In the present study, the particle size of RSV was reduced by the temperature-controlled antisolvent precipitation method. Further, characterization of the NRSV was done by SEM and *in vitro* dissolution test to evaluate the size of the particles and dissolution rate. The SEM analysis of NRSV revealed the formation of nanoparticles, showed the spherical shape, and found to be within the range of 100–250 nm. In addition to that, *in vitro* dissolution study of NRSV has shown high dissolution rate as compared to the commercial RSV which may be attributed to the fact that the size reduction of a poorly water-soluble compound to nanoparticles results in increased surface specific dissolution rate.[39,40] Here, we can conclude that the higher dissolution rate of NRSV resulted from the decreased particle size and could translate into increased bioavailability. Therefore, the increased bioavailability of RSV leads to enhancement of pharmacokinetic interaction with the concomitantly administered BRO which results in change in the total exposure of the BRO in the body and reflects in improved blood concentration.

Here, we explored the influence of RSV on EMD assay, which is an indicator of CYP3A activity. The results indicate that RSV inhibited the CYP3A activity in intestinal microsomes to a greater extent than the liver microsomes; it is due to the fact that intestinal microsomal preparations have a low overall concentration of CYPs in comparison to hepatic preparations.[24] These results are in accordance with the earlier reports, i.e., RSV enhanced the bioavailability of CYP3A4 substrates such as carbamazepine[16] and diltiazem[5] by CYP3A inhibition in rats. Considering that BRO is a substrate of CYP enzymes and inhibitory action on CYP may cause significant changes in the pharmacokinetic profile of BRO.

It has been clearly demonstrated that CYP3A4 is the predominant CYP form expressed in the human small intestine.[41-43] Orally administered xenobiotics, including therapeutic drugs initially metabolized in the enterocytes, epithelial cells of the human small intestine.[44] Toxicity and therapeutic efficacy of orally administered xenobiotics are substantially affected by the small intestinal CYP metabolism. Early studies reported that rifampin[41] induced the action of CYP3A4 by increasing human intestinal expression. In addition, constituents of grapefruit juice significantly increase the uptake of drugs such as felodipine,[45] saquinavir,[46] and ethinylestradiol[47] by decreasing the intestinal expression of CYP3A4.

In this study, the intestinal transport and P_{app} of BRO were significantly increased in duodenum, jejunum, and ileal sacs of rats pretreated with RSV and NRSV as compared to control group. The intestinal transport and P_{app} of BRO were more prominent in rats pretreated with NRSV than RSV-pretreated animals. Pretreatment with RSV and NRSV increased the P_{app} of BRO in rats, in the order duodenum > jejunum > ileum. We have found that our results are consistent with a study reported by Zhang *et al*.[48] Microsomal protein content decreased markedly along the small intestine from the duodenum to the ileum. Therefore, these studies further confirm the inhibitory action of RSV and NRSV on CYP3A activity.

Further, we also performed *in vivo* studies in rats to support *in vitro* liver and intestinal CYP3A activity and *in vitro* intestinal transport of BRO in noneverted sac model. Here, we evaluated the effect of RSV and NRSV on the metabolism and pharmacokinetics of BRO. RSV and NRSV pretreatment for 10 days increased the oral bioavailability of BRO in rats. RSV and NRSV groups have shown significant increase in the C_{max} and AUC when compared to BRO group suggesting that pretreatment of RSV and NRSV for 10 days significantly altered pharmacokinetics and enhanced bioavailability of BRO. In addition, pretreatment with RSV and NRSV resulted in a significant decrease in mean CL/F of BRO while there was no significant change observed in t_{max} of BRO when compared to BRO group. Decreased CL/F, k_{el} and increased $t_{1/2}$ values indicating the inhibition of elimination of BRO

upon RSV and NRSV pretreatment. Here, we observed that NRSV-pretreated group has shown the more prominent results than RSV pretreated group, which indicates improved therapeutic efficacy of NRSV.

Conclusion

The results of the present study revealed that NRSV pretreatment significantly increased the intestinal absorption and bioavailability of BRO probably by the inhibition of CYP3A-mediated metabolism in rats. Therefore, the inhibition of CYP3A by dietary phytochemicals such as NRSV may provide a novel therapeutic approach for the clinical application which could improve the efficacy, reduce the incidence of side effects, and allow the optimal therapeutic dosing of BRO. However, further studies are necessary to conclude phytochemical-mediated CYP3A4 interactions with BRO in humans.

Acknowledgments

This research received no specific grant from any funding agency in the public, commercial, or not-for-profit sectors. University College of pharmaceutical sciences, Kakatiya University, support for the routine reagents, and permission to animal holding for this research. Authors would like to thank Inga laboratories Pvt. Ltd., Maharashtra, for providing BRO as a gift sample.

Financial support and sponsorship

Nil.

Conflicts of interest

There are no conflicts of interest.

References

1. Chen RS, Wu PL, Chiou RY. Peanut roots as a source of resveratrol. J Agric Food Chem 2002;50:1665-7.
2. Queiroz AN, Gomes BA, Moraes WM Jr., Borges RS. A theoretical antioxidant pharmacophore for resveratrol. Eur J Med Chem 2009;44:1644-9.
3. Sánchez-Fidalgo S, Cárdeno A, Villegas I, Talero E, de la Lastra CA. Dietary supplementation of resveratrol attenuates chronic colonic inflammation in mice. Eur J Pharmacol 2010;633:78-84.
4. Zykova TA, Zhu F, Zhai X, Ma WY, Ermakova SP, Lee KW, *et al.* Resveratrol directly targets COX-2 to inhibit carcinogenesis. Mol Carcinog 2008;47:797-805.
5. Hong SP, Choi DH, Choi JS. Effects of resveratrol on the pharmacokinetics of diltiazem and its major metabolite, desacetyldiltiazem, in rats. Cardiovasc Ther 2008;26:269-75.
6. Zhan YY, Liang BQ, Li XY, Gu EM, Dai DP, Cai JP, *et al.* The effect of resveratrol on pharmacokinetics of aripiprazole *in vivo* and *in vitro*. Xenobiotica 2016;46:439-44.
7. Chang TK, Yeung RK. Effect of trans-resveratrol on 7-benzyloxy-4-trifluoromethylcoumarin O-dealkylation catalyzed by human recombinant CYP3A4 and CYP3A5. Can J Physiol Pharmacol 2001;79:220-6.
8. Chan WK, Delucchi AB. Resveratrol, a red wine constituent, is a mechanism-based inactivator of cytochrome P450 3A4. Life Sci 2000;67:3103-12.
9. Yu C, Shin YG, Kosmeder JW, Pezzuto JM, van Breemen RB. Liquid chromatography/tandem mass spectrometric determination of inhibition of human cytochrome P450 isozymes by resveratrol and resveratrol-3-sulfate. Rapid Commun Mass Spectrom 2003;17:307-13.
10. Hao J, Gao Y, Zhao J, Zhang J, Li Q, Zhao Z, *et al.* Preparation and optimization of resveratrol nanosuspensions by antisolvent precipitation using box-behnken design. AAPS PharmSciTech 2015;16:118-28.
11. Shindikar A, Singh A, Nobre M, Kirolikar S. Curcumin and resveratrol as promising natural remedies with nanomedicine approach for the effective treatment of triple negative breast cancer. J Oncol 2016;2016:9750785.
12. Dokoumetzidis A, Macheras P. A century of dissolution research: From Noyes and Whitney to the biopharmaceutics classification system. Int J Pharm 2006;321:1-1.
13. Wang E, Lew K, Barecki M, Casciano CN, Clement RP, Johnson WW. Quantitative distinctions of active site molecular recognition by P-glycoprotein and cytochrome P450 3A4. Chem Res Toxicol 2001;14:1596-603.
14. Fakhoury M, Litalien C, Medard Y, Cavé H, Ezzahir N, Peuchmaur M, *et al.* Localization and mRNA expression of CYP3A and P-glycoprotein in human duodenum as a function of age. Drug Metab Dispos 2005;33:1603-7.
15. Wilkinson GR. Cytochrome P4503A (CYP3A) metabolism: Prediction of *in vivo* activity in humans. J Pharmacokinet Biopharm 1996;24:475-90.
16. Bedada SK, Nearati P. Effect of resveratrol on the pharmacokinetics of carbamazepine in healthy human volunteers. Phytother Res 2015;29:701-6.
17. Defronzo RA. Bromocriptine: A sympatholytic, d2-dopamine agonist for the treatment of type 2 diabetes. Diabetes Care 2011;34:789-94.
18. Md S, Haque S, Fazil M, Kumar M, Baboota S, Sahni JK, *et al.* Optimised nanoformulation of bromocriptine for direct nose-to-brain delivery: Biodistribution, pharmacokinetic and dopamine estimation by ultra-HPLC/mass spectrometry method. Expert Opin Drug Deliv 2014;11:827-42.
19. Viney L, Dharmpal S, Deepti P. Proniosomal gel-mediated transdermal delivery of bromocriptine: *In vitro* and *ex vivo* evaluation. J Exp Nanosci 2016;11:1044-57.
20. Nelson MV, Berchou RC, Kareti D, LeWitt PA. Pharmacokinetic evaluation of erythromycin and caffeine administered with bromocriptine. Clin Pharmacol Ther 1990;47:694-7.
21. Maurer G, Schreier E, Delaborde S, Nufer R, Shukla AP. Fate and disposition of bromocriptine in animals and man. II: Absorption, elimination and metabolism. Eur J Drug Metab Pharmacokinet 1983;8:51-62.
22. Davydov DR, Halpert JR, Renaud JP, Hui Bon Hoa G. Conformational heterogeneity of cytochrome P450 3A4 revealed by high pressure spectroscopy. Biochem Biophys Res Commun 2003;312:121-30.
23. Via MA, Chandra H, Araki T, Potenza MV, Skamagas M. Bromocriptine approved as the first medication to target dopamine activity to improve glycemic control in patients with type 2 diabetes. Diabetes Metab Syndr Obes 2010;3:43-8.
24. Cao X, Gibbs ST, Fang L, Miller HA, Landowski CP, Shin HC, *et al.* Why is it challenging to predict intestinal drug absorption and oral bioavailability in human using rat model. Pharm Res 2006;23:1675-86.
25. Kim S, Ng WK, Dong Y, Das S, Tan RB. Preparation and physicochemical characterization of trans-resveratrol nanoparticles by temperature-controlled antisolvent precipitation. J Food Eng 2012;108:37-42.
26. Shantha KL, Harding DR. Preparation and *in vitro* evaluation of poly[N-vinyl-2-pyrrolidone-polyethylene glycol diacrylate]-chitosan interpolymeric pH-responsive hydrogels for oral drug delivery. Int J Pharm 2000;207:65-70.
27. Samala S, Veeresham C. Pharmacokinetic and pharmacodynamic interaction of boswellic acids and andrographolide with glyburide in diabetic rats: Including its PK/PD modeling. Phytother Res 2016;30:496-502.
28. Nash T. The colorimetric estimation of formaldehyde by means of the Hantzsch reaction. Biochem J 1953;55:416-21.
29. Cotreau MM, von Moltke LL, Beinfeld MC, Greenblatt DJ. Methodologies to study the induction of rat hepatic and intestinal cytochrome P450 3A at the mRNA, protein, and catalytic activity level. J Pharmacol Toxicol Methods 2000;43:41-54.
30. Takemoto K, Yamazaki H, Tanaka Y, Nakajima M, Yokoi T.

Catalytic activities of cytochrome P450 enzymes and UDP-glucuronosyltransferases involved in drug metabolism in rat everted sacs and intestinal microsomes. Xenobiotica 2003;33:43-55.
31. Schenkman JB, Cinti DL. Preparation of microsomes with calcium. Methods Enzymol 1978;52:83-9.
32. Neerati P, Bedada SK. Effect of diosmin on the intestinal absorption and pharmacokinetics of fexofenadine in rats. Pharmacol Rep 2015;67:339-44.
33. Wada S, Kano T, Mita S, Idota Y, Morimoto K, Yamashita F, *et al.* The role of inter-segmental differences in P-glycoprotein expression and activity along the rat small intestine in causing the double-peak phenomenon of substrate plasma concentration. Drug Metab Pharmacokinet 2013;28:98-103.
34. Ruan LP, Chen S, Yu BY, Zhu DN, Cordell GA, Qiu SX. Prediction of human absorption of natural compounds by the non-everted rat intestinal sac model. Eur J Med Chem 2006;41:605-10.
35. Choi YJ, Seo MK, Kim IC, Lee YH. High-performance liquid chromatographic assay of bromocriptine in plasma and eye tissue of the rabbit. J Chromatogr B Biomed Sci Appl 1997;694:415-20.
36. Evans AM. Influence of dietary components on the gastrointestinal metabolism and transport of drugs. Ther Drug Monit 2000;22:131-6.
37. Wilkinson GR. The effects of diet, aging and disease-states on presystemic elimination and oral drug bioavailability in humans. Adv Drug Deliv Rev 1997;27:129-59.
38. Meng Q, Liu K. Pharmacokinetic interactions between herbal medicines and prescribed drugs: Focus on drug metabolic enzymes and transporters. Curr Drug Metab 2014;15:791-807.
39. Mosharrafand M, Nystrom C. The effect of particle size and shape on the surface specific dissolution rate of microsized practically insoluble drugs. Int J Pharm 1995;122:35-47.
40. Kesisoglou F, Panmai S, Wu Y. Nanosizing – Oral formulation development and biopharmaceutical evaluation. Adv Drug Deliv Rev 2007;59:631-44.
41. Kolars JC, Schmiedlin-Ren P, Schuetz JD, Fang C, Watkins PB. Identification of rifampin-inducible P450IIIA4 (CYP3A4) in human small bowel enterocytes. J Clin Invest 1992;90:1871-8.
42. Peters WH, Kremers PG. Cytochromes P-450 in the intestinal mucosa of man. Biochem Pharmacol 1989;38:1535-8.
43. de Waziers I, Cugnenc PH, Yang CS, Leroux JP, Beaune PH. Cytochrome P 450 isoenzymes, epoxide hydrolase and glutathione transferases in rat and human hepatic and extrahepatic tissues. J Pharmacol Exp Ther 1990;253:387-94.
44. Paine MF, Shen DD, Kunze KL, Perkins JD, Marsh CL, McVicar JP, *et al.* First-pass metabolism of midazolam by the human intestine. Clin Pharmacol Ther 1996;60:14-24.
45. Lown KS, Bailey DG, Fontana RJ, Janardan SK, Adair CH, Fortlage LA, *et al.* Grapefruit juice increases felodipine oral availability in humans by decreasing intestinal CYP3A protein expression. J Clin Invest 1997;99:2545-53.
46. Kupferschmidt HH, Fattinger KE, Ha HR, Follath F, Krähenbühl S. Grapefruit juice enhances the bioavailability of the HIV protease inhibitor saquinavir in man. Br J Clin Pharmacol 1998;45:355-9.
47. Weber A, Jäger R, Börner A, Klinger G, Vollanth R, Matthey K, *et al.* Can grapefruit juice influence ethinylestradiol bioavailability? Contraception 1996;53:41-7.
48. Zhang QY, Dunbar D, Ostrowska A, Zeisloft S, Yang J, Kaminsky LS. Characterization of human small intestinal cytochromes P-450. Drug Metab Dispos 1999;27:804-9.